Department of Pharmaceutics[1], Faculty of Pharmaceutical Sciences, Hokkaido University of Science, Creation Research Institute of Life Science in KITA-no-DAICHI[2], Sapporo, Japan

Assessment of transporter-mediated efflux of nintedanib using *in vitro* cell line models of idiopathic pulmonary fibrosis

K. Togami[1,2,*], K. Yamaguchi[1], H. Tada[1], S. Chono[1,2]

Received April 9, 2020, accepted June 6, 2020

**Corresponding author: Kohei Togami, PhD, Department of Pharmaceutics, Faculty of Pharmaceutical Sciences, Hokkaido University of Science, 7-Jo 15-4-1 Maeda, Teine, Sapporo, Hokkaido 006-8585, Japan*
k-togami@hus.ac.jp

Pharmazie 75: 371-374 (2020) *doi: 10.1691/ph.2020.0048*

Objective: We aimed to investigate the involvement of efflux transporters, including multidrug resistant protein 1 (MDR1), multidrug resistance-associated protein 1 (MRP1), MRP2, and breast cancer resistance protein (BCRP), in the intracellular accumulation of the antifibrotic agent nintedanib in fibrotic lung cells. *Methods:* We used transforming growth factor-β_1 (TGF-β_1)-treated human lung fibroblasts (WI-38) and alveolar epithelial cells (A549) as *in vitro* models. The expression and activities of efflux transporters in TGF-β_1-treated WI-38 and A549 cells were evaluated using immunoblotting and flow cytometry. Cells were treated with nintedanib and then incubated with inhibitors of these transporters. The intracellular concentration of nintedanib was determined. *Results:* MDR1, MRP1, MRP2, and BCRP were found to be expressed in WI-38 and A549 cells with or without TGF-β_1 stimulation, with the exception of MRP2 in WI-38 cells. The efflux activities of these transporters were observed in these cells. MDR1 inhibitors significantly increased the intracellular accumulation of nintedanib, whereas MRP inhibitors did not show an effect. The BCRP inhibitor significantly increased the transporter activity in A549 cells but not in WI-38 cells. *Conclusion:* This study suggests that the efflux via MDR1 and BCRP is involved in the intracellular accumulation of nintedanib in fibrotic lung cells.

1. Introduction

Idiopathic pulmonary fibrosis (IPF) is a chronic, progressive, and fibrotic lung disease. IPF is associated with poor quality of life, respiratory insufficiency, and short survival time from diagnosis (2–4 years) (Kistler et al. 2014; Ley et al. 2011; Yount et al. 2016). IPF pathology is characterized by abnormal repetitive alveolar epithelium injury and repair. This results in the aberrant accumulation of the extracellular matrix produced by lung fibroblasts and myofibroblasts (Borensztajn et al. 2013; Richeldi et al. 2017). The pathological features of IPF are caused by fibrogenic mediators, particularly transforming growth factor-β_1 (TGF-β_1). TGF-β_1 stimulation contributes to IPF progression through fibroblast proliferation, migration, and fibroblasts differentiation into activated myofibroblasts (FMT) (Fernandez and Eickelberg 2012). In addition, the epithelial to mesenchymal transition (EMT) induced by TGF-β_1 stimulation in alveolar epithelial cells contributes to IPF progression (Salton et al. 2019).

Nintedanib, an antifibrotic agent, is clinically used for the treatment of IPF in the EU (Vargatef®), Japan, Switzerland, and the US (OFEV®) (Mazzei et al. 2015; McCormack 2015). Nintedanib inhibits multiple receptors of pro-fibrotic growth factors, including fibroblast growth factor receptor (FGFR), vascular endothelial growth factor receptor (VEGFR), and platelet-derived growth factor receptor (PDGFR). Nintedanib acts *via* competitive binding to the ATP-binding pocket of the intracellular kinase domain of these receptors (Hilberg et al. 2008). As a result, nintedanib has good antifibrotic efficacy and inhibition effects on proliferation, migration, FMT, and EMT. Through these activities, nintedanib inhibits collagen secretion (Hilberg et al. 2008; Li et al. 2017; Wollin et al. 2014).

A previous *in vitro* study suggested that nintedanib is a substrate of multidrug resistant protein 1 (MDR1) and breast cancer resistance protein (BCRP) efflux transporters (FDA Center for Drug Evaluation and Research, Nintedanib clinical pharmacology NDA review, Application number: 205832Orig1s000). In addition, the oral bioavailability of nintedanib is increased by the co-administration of the MDR1 inhibitor ketoconazole and decreased by the co-administration of the MDR1 inducer rifampicin (Luedtke et al. 2018). Thus, the activities of efflux transporters in fibrotic lung cells, including lung fibroblasts, myofibroblasts, and mesenchymal cells, may interfere with the intracellular accumulation of nintedanib and undermine its antifibrotic effect. However, the involvement of efflux transporters in the intracellular accumulation of nintedanib in fibrotic lung cells remains largely unknown. In this study, we established *in vitro* models of fibrotic lung cells using TGF-β_1-treated and non-treated human lung fibroblasts (WI-38) and alveolar epithelial cells (A549). We utilized these models for the evaluation of the expression and activity of efflux transporters, including MDR1, multidrug resistance-associated protein 1 (MRP1), MRP2, and BCRP. Additionally, the involvement of these efflux transporters in the intracellular accumulation of nintedanib was evaluated using these models.

2. Investigations and results

2.1. TGF-β_1-induced FMT and EMT

The morphology and marker expressions of TGF-β_1-treated WI-38 and A549 cells are shown in Fig. 1. The morphological change induced by TGF-β_1 was observed in both WI-38 and A549 cells. In addition, TGF-β_1 treatment significantly increased the expression of the myofibroblast marker α-smooth muscle actin (SMA) in WI-38 cells and the expression of the mesenchymal marker vimentin in A549 cells. TGF-β_1 treatment significantly decreased the expression of the epithelial marker E-cadherin in A549 cells.

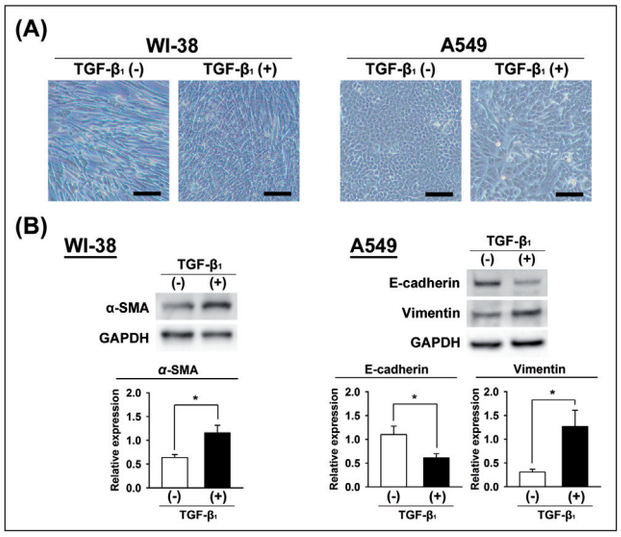

Fig. 1: TGF-β_1-induced fibroblast differentiation into activated myofibroblasts (FMT), myofibroblast differentiation, and epithelial mesenchymal transition (EMT) *in vitro* models. (A) Morphologic characteristics of WI-38 and A549 cells with or without TGF-β_1 (10 ng/mL) treatment for 24 h. Scale bar = 200 µm. (B) Immunoblotting images demonstrating marker expression in WI-38 and A549 cells with or without TGF-β_1 (10 ng/mL) treatment for 24 h. α-SMA is a myofibroblast marker in WI-38 cells. E-cadherin and vimentin are epithelial and mesenchymal markers in A549 cells, respectively. The densities of bands were normalized using GAPDH and expressed as ratios of band intensities. Each point represents the mean±S.D. (n = 3). $*p < 0.01$. The data for A549 cells are taken from published literature (Togami et al. 2017).

2.2. *Expression of efflux transporters*

The expression profiles of MDR1, MRP1, MRP2, and BCRP in cells are shown in Fig. 2. Efflux transporters were detected in WI-38 and A549 cells with or without TGF-β_1 treatment, with the exception of MRP2 in WI-38 cells. Transporter expression was not changed by TGF-β_1 treatment.

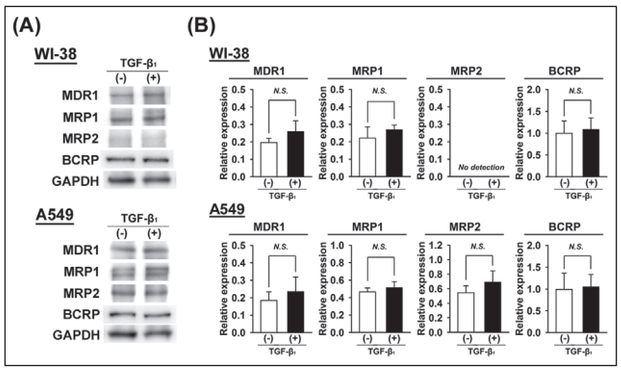

Fig. 2: Expression of efflux transporters in WI-38 and A549 cells with or without TGF-β_1 treatment. (A) Immunoblotting images demonstrating MDR1, MRP1/2, and BCRP protein accumulation in WI-38 and A549 cells with or without TGF-β_1 (10 ng/mL) treatment for 24 h. (B) The densities of bands were normalized using GAPDH and expressed as ratios of intensities. Each point represents the mean±S.D. (n = 3). N.S.: Not significant.

2.3. *Efflux activities of efflux transporters*

The efflux activities of the transporters in cells are shown in Fig. 3. The histograms of eFluxx-ID fluorescent intensities demonstrated increased signal in the presence of the inhibitors of each efflux transporter. The multidrug resistance activity factor (MAF) values for MDR1, MRP1/2, and BCRP in each cell were greater than 25, indicating positivity of transporter activities.

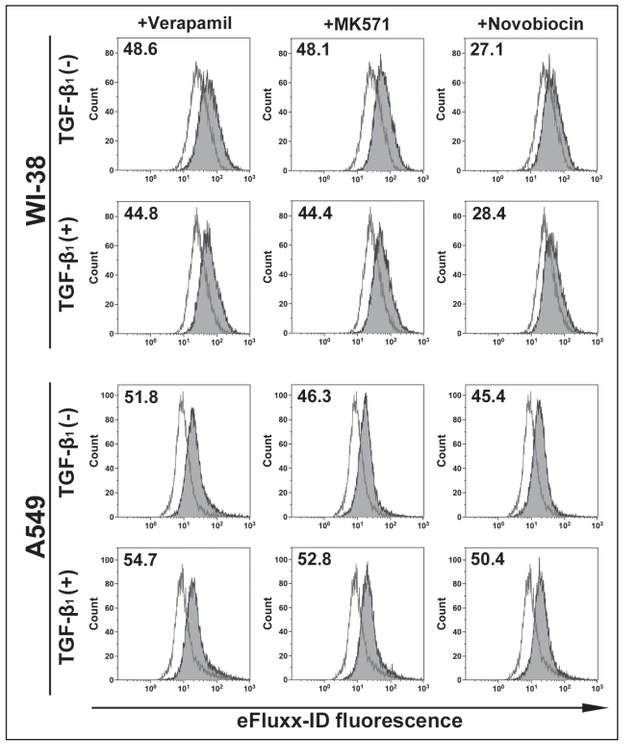

Fig. 3: The eFluxx-ID assay for activities of efflux transporters in WI-38 and A549 cells with or without TGF-β_1 treatment. Verapamil, MK571, and novobiocin were used for MDR1, MRP1/2, and BCRP inhibition, respectively. White histograms represent control samples, and gray histograms represent samples treated with each inhibitor. The MAF scores in the upper left corners of each panel were calculated using three samples per group and formula 1.

2.4. *Effects of efflux transporter inhibitors on the intracellular accumulation of nintedanib*

The intracellular accumulation of nintedanib in cells in the presence of efflux transporter inhibitors is shown in Fig. 4. The MDR1 inhibitor GF120918 significantly increased the intracellular accumulation of nintedanib in TGF-β_1-treated and non-treated WI-38 and A549 cells. The BCRP inhibitor Ko143 significantly increased the intracellular accumulation of nintedanib in TGF-β_1-treated and non-treated A549 cells. The MRP1/2 inhibitor MK-571 did not change the intracellular accumulation of nintedanib.

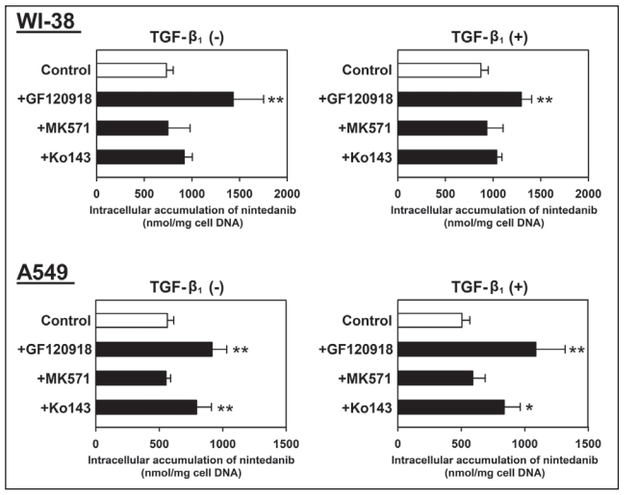

Fig. 4: Effects of inhibitors on the intracellular accumulation of nintedanib in WI-38 and A549 cells with or without TGF-β_1 treatment. Nintedanib (3 µM) was applied to cells in the presence of the MDR1 inhibitor GF120918 (10 µM), the MRP1/2 inhibitor MK571 (20 µM), or the BCRP inhibitor Ko143 (10 µM). After a 2 h incubation, the intracellular concentration of nintedanib was determined. Each point represents the mean±S.D. (n = 4). $*p < 0.05$, $**p < 0.01$.

3. Discussion

In this study, we demonstrated the involvement of efflux transporters in the intracellular accumulation of nintedanib in fibrotic lung cells using *in vitro* models. First, we demonstrated TGF-β_1-induced FMT and EMT of lung cell lines (WI-38 and A549) (Fig. 1). Similarly, other researchers used TGF-β_1-treated WI-38 and A549 cells as *in vitro* models of FMT and EMT for pharmacological studies of pulmonary fibrosis (Li et al. 2018; Schruf et al. 2019; Sun et al. 2019; Yamazaki et al. 2017). However, the expression and activities of efflux transporters in TGF-β_1-treated cells has not been reported. In this study, we clarified the expression and activities of efflux transporters in TGF-β_1-treated and non-treated WI-38 and A549 cells (Figs. 2 and 3). Park et al. (2019) reported that MDR1 and BCRP were expressed in multiple types of lung cells, including alveolar epithelial cells, lung fibroblasts, and myofibroblasts, in IPF patients. These findings indicated that TGF-β_1-treated and non-treated WI-38 and A549 cells are useful as *in vitro* models of fibrotic lung cells for the evaluation of efflux transporter involvement in intracellular drug accumulation.

Experimental animal models with bleomycin-induced pulmonary fibrosis are widely used to study IPF pathogenesis and for the development of IPF therapies. However, although the expression levels of MDR1 and BCRP did not change during human IPF progression, they were enhanced in experimental animals with bleomycin-induced pulmonary fibrosis (Park et al. 2019). The upregulation of efflux activities in the fibrotic lung cells of experimental animal models interferes with pharmacological actions via the reduction of the accumulation of their substrate drugs in cells. This may lead to inaccurate interpretation of pharmacological activities in animal studies and, consequently, false-negative results. Therefore, TGF-β_1-treated WI-38 and A549 cells may be suitable for the evaluation of the distribution characteristics of efflux transporter substrates in fibrotic cells.

In the current study, nintedanib was exported actively by MDR1 on TGF-β_1-treated and non-treated WI-38 and A549 cells and by BCRP on TGF-β_1-treated and non-treated A549 cells (Fig. 4). Since the pharmacological effects of tyrosine kinase inhibitors such as nintedanib occur *via* binding to intracellular target molecules, the efflux characteristics of these drugs determine their efficacies (de Klerk et al. 2018). In addition, the plasma concentration profiles of nintedanib were altered by the co-administration of an MDR1 inhibitor or inducer (Luedtke et al. 2018). These findings suggest that the antifibrotic effect of nintedanib on fibrotic lung cells is altered with the co-administration of MDR1 and BCRP inhibitors or inducers *via* changes in intracellular accumulation and circulatory tissue distribution. Many tyrosine kinase inhibitors are known to be MDR1 and/or BCRP substrates (Da Silva et al. 2015; de Klerk et al. 2018; Neul et al. 2016). Currently, multiple novel tyrosine kinase inhibitors with antifibrotic effects are being developed for more effective IPF treatment with less toxicity (Koyama et al. 2019; Ruan et al. 2020; Sun et al. 2020). To accurately understand the pharmacokinetics and pharmacodynamics of novel tyrosine kinase inhibitors, it may be necessary to evaluate their efflux activities in fibrotic lung cells. This may be accomplished with *in vitro* models using TGF-β_1-treated and non-treated WI-38 and A549 cells.

In conclusion, the expression and functions of MDR1, MRP1, MRP2, and BCRP on TGF-β_1-treated and non-treated WI-38 and A549 cells were examined using *in vitro* fibrotic lung cell models. In addition, the efflux of nintedanib *via* these transporters was evaluated in these cells. This study indicates that TGF-β_1-treated and non-treated WI-38 and A549 cells are useful for the study of the accumulation of efflux transporter substrates in fibrotic lung cells.

4. Experimental

4.1. Materials

Nintedanib was purchased from ChemScene Llc. (Monmouth Junction, NJ, USA). GF120918 and MK571 were purchased from Cayman Chemical Co. (Ann Arbor, MI, USA). Ko143 was purchased from Enzo Life Sciences, Inc. (Farmingdale, NY, USA). All other reagents were commercially available and of analytical grade.

4.2. Cell culture

WI-38 (Riken Cell Bank, Tsukuba, Japan) and A549 (Riken Cell Bank) cells were maintained in Dulbecco's modified Eagle's medium (DMEM) containing 10% heat-inactivated fetal bovine serum (FBS) and 40 µg/mL gentamicin. WI-38 and A549 cells of passage numbers 11–15 and 95–99 were used, respectively. The cells were maintained in a humidified atmosphere with 5% CO_2 at 37 °C.

4.3. Immunoblotting

Immunoblotting was performed as described previously (Togami et al. 2017). In brief, TGF-β_1 (10 ng/mL) was applied to WI-38 and A549 cells, which were incubated for an additional 24 h at 37 °C in 5% CO_2. Protein in cell lysates was separated by sulfate-polyacrylamide gel electrophoresis using 4–15% gradient gels (5 µg protein/lane). Proteins were transferred to polyvinylidene difluoride membranes (20 V, 60 min), and 0.1% Tween 20 and 5% non-fat milk were used for blocking overnight at 4 °C. The membranes were incubated with mouse monoclonal anti-α-SMA antibody (Sigma Aldrich Co., St. Louis, MO, USA, Catalog number: A2547, 1;400 dilution), mouse monoclonal anti-vimentin antibody (Abcam plc, Cambridge, UK, Catalog number: ab8978, 1:250 dilution), rabbit polyclonal anti-E-cadherin antibody (Sigma Aldrich, Catalog number: HPA004812, 1:250 dilution), mouse monoclonal anti-MDR1 antibody (GeneTex Inc., Irvine, CA, USA, Catalog number: GTX23364, 1:50), mouse monoclonal anti-MRP1 antibody (Kamiya Biomedical Co., Seattle, WA, USA, Catalog number: MC-162, 1:50 dilution), rabbit polyclonal anti-MRP2 antibody (Sigma Aldrich, Catalog number: M8316, 1:1000 dilution), rabbit monoclonal anti-BCRP antibody (Abcam, Catalog number: ab108312, 1:1000), or rabbit monoclonal anti-GAPDH antibody (Abcam, Catalog number: ab181602, 1:10000 dilution) for 1 h at room temperature. For the evaluation of protein expression, membranes were incubated with horseradish peroxidase-conjugated antimouse or antirabbit IgG secondary antibodies (GE Healthcare, Pollards Wood, UK, 1:2000 dilution). Antibody–protein complexes were detected using an enhanced chemiluminescence assay (Bio-Rad, Hercules, CA, USA). Relative levels of protein expression were quantified using band densities as determined with ImageJ software version 1.52 (National Institutes of Health, Bethesda, MD, USA).

4.4. Efflux activity assay

Efflux activity assays were performed on WI-38 and A549 cells using flow cytometry. After TGF-β_1 (10 ng/mL) treatment for 24 h at 37 °C, cells were harvested by trypsinization. Efflux activities were evaluated using the eFluxx-ID™ green multidrug resistance assay kit (Enzo Life Sciences) according to the kit manual. In brief, eFluxx-ID green detection reagent was applied to cells in the presence of 20 µM verapamil, 50 µM MK571, or 100 µM novobiocin. Cells were incubated for 2 h at 37 °C. Treated cells were analyzed using flow cytometry (Gallios; Beckman Coulter, Fullerton, CA, USA). The mean fluorescence intensities (MFI) of eFluxx-ID green in the cells were obtained using Kaluza software version 2.1 (Beckman Coulter). The multidrug resistance activity factor (MAF) for each transporter was calculated using Eq. (1):

$$MAF = \frac{MFI_{etr} - MFI_{cont}}{MFI_{etr}} \times 100, \qquad (1)$$

where MFI_{etr} is the MFI in the presence of the inhibitor for each efflux transporter and MFI_{cont} is the MFI of the negative control.

4.5. Nintedanib accumulation experiments

WI-38 and A549 cells were seeded on 48-well culture plates (5.0×10^4 cells/well) and incubated for 48 h at 37 °C with 5% CO_2. Cells were then incubated with TGF-β_1 (10 ng/mL) for an additional 24 h at 37 °C in 5% CO_2. Nintedanib (3 µM) was applied to cells in the presence of 10 µM GF120918, 50 µM MK571, or 10 µM Ko143, and cells were incubated for 2 h at 37 °C. Media were removed by aspiration, and cells were washed three times with ice-cold PBS. Cellular contents were then extracted using 400 µL of 2 M NaCl. Nintedanib concentrations in the cell extracts were measured using HPLC as reported previously (Togami et al. 2018). The DNA concentrations in the cell extracts were determined using a Fluorescent DNA Quantitation Kit (Bio-Rad).

4.6. Statistical analysis

Statistical analyses were carried out using the Student t-test and Dunnett's test with SPSS software version 24 (IBM Inc., Armonk, NY, USA). A p-value of <0.05 was considered to indicate statistical significance.

Acknowledgments: This work was supported by JSPS KAKENHI Grant Numbers JP17H02178, JP18K06603, and JP18K12066 provided by the Japan Society for the Promotion of Science, a grant (number H29ST-ST-36) provided by Northern Advancement Center for Science and Technology (Sapporo, Japan), and a Grant-in-Aid (2019) provided by The Akiyama Life Science Foundation (Sapporo, Japan).

Conflicts of interest: None declared.

References

Borensztajn K, Crestani B, Kolb M (2013) Idiopathic pulmonary fibrosis: from epithelial injury to biomarkers--insights from the bench side. Respiration 86: 441–452.

Da Silva CG, Honeywell RJ, Dekker H, Peters GJ (2015) Physicochemical properties of novel protein kinase inhibitors in relation to their substrate specificity for drug transporters. Expert Opin Drug Metab Toxicol 11: 703–717.

de Klerk DJ, Honeywell RJ, Jansen G, Peters GJ (2018) Transporter and lysosomal mediated (multi)drug resistance to tyrosine kinase inhibitors and potential strategies to overcome resistance. Cancers 10: 503.

Fernandez IE, Eickelberg O (2012) The impact of TGF-beta on lung fibrosis: from targeting to biomarkers. Proc Am Thorac Soc 9: 111–116.

Hilberg F, Roth GJ, Krssak M, Kautschitsch S, Sommergruber W, Tontsch-Grunt U, Garin-Chesa P, Bader G, Zoephel A, Quant J, Heckel A, Rettig WJ (2008) BIBF 1120: triple angiokinase inhibitor with sustained receptor blockade and good antitumor efficacy. Cancer Res 68: 4774–4782.

Kistler KD, Nalysnyk L, Rotella P, Esser D (2014) Lung transplantation in idiopathic pulmonary fibrosis: a systematic review of the literature. BMC Pulm Med 14: 139.

Koyama K, Goto H, Morizumi S, Kagawa K, Nishimura H, Sato S, Kawano H, Toyoda Y, Ogawa H, Homma S, Nishioka Y (2019) The tyrosine kinase inhibitor TAS-115 attenuates bleomycin-induced lung fibrosis in mice. Am J Respir Cell Mol Biol 60: 478–487.

Ley B, Collard HR, King TE, Jr. (2011) Clinical course and prediction of survival in idiopathic pulmonary fibrosis. Am J Respir Crit Care Med 183: 431–440.

Li LF, Kao KC, Liu YY, Lin CW, Chen NH, Lee CS, Wang CW, Yang CT (2017) Nintedanib reduces ventilation-augmented bleomycin-induced epithelial-mesenchymal transition and lung fibrosis through suppression of the Src pathway. J Cell Mol Med 21: 2937–2949.

Li XH, Xiao T, Yang JH, Qin Y, Gao JJ, Liu HJ, Zhou HG (2018) Parthenolide attenuated bleomycin-induced pulmonary fibrosis via the NF-kappaB/Snail signaling pathway. Respir Res 19: 111.

Luedtke D, Marzin K, Jungnik A, von Wangenheim U, Dallinger C (2018) Effects of ketoconazole and rifampicin on the pharmacokinetics of nintedanib in healthy subjects. Eur J Drug Metab Pharmacokinet 43: 533–541.

Mazzei ME, Richeldi L, Collard HR (2015) Nintedanib in the treatment of idiopathic pulmonary fibrosis. Ther Adv Respir Dis 9: 121–129.

McCormack PL (2015) Nintedanib: first global approval. Drugs 75: 129–139.

Neul C, Schaeffeler E, Sparreboom A, Laufer S, Schwab M, Nies AT (2016) Impact of membrane drug transporters on resistance to small-molecule tyrosine kinase inhibitors. Trends Pharmacol Sci 37: 904–932.

Park JK, Coffey NJ, Bodine SP, Zawatsky CN, Jay L, Gahl WA, Kunos G, Gochuico BR, Malicdan MCV, Cinar R (2019) Bleomycin induces drug efflux in lungs: A pitfall for pharmacological studies of Pulmonary Fibrosis. Am J Respir Cell Mol Biol 62: 178–190.

Richeldi L, Collard HR, Jones MG (2017) Idiopathic pulmonary fibrosis. Lancet 389: 1941–1952.

Ruan H, Lv Z, Liu S, Zhang L, Huang K, Gao S, Gan W, Liu X, Zhang S, Helian K, Li X, Zhou H, Yang C (2020) Anlotinib attenuated bleomycin-induced pulmonary fibrosis via the TGF-beta1 signalling pathway. J Pharm Pharmacol 72: 44–55.

Salton F, Volpe MC, Confalonieri M (2019) Epithelial(-)mesenchymal transition in the pathogenesis of idiopathic pulmonary fibrosis. Medicina (Kaunas) 55: 83.

Schruf E, Schroeder V, Kuttruff CA, Weigle S, Krell M, Benz M, Bretschneider T, Holweg A, Schuler M, Frick M, Nicklin P, Garnett JP, Sobotta MC (2019) Human lung fibroblast-to-myofibroblast transformation is not driven by an LDH5-dependent metabolic shift towards aerobic glycolysis. Respir Res 20: 87.

Sun B, Liu X, Zheng X, Wang C, Meng Q, Sun H, Shu X, Liu K, Sun X, Li Y, Ma X (2020) Novel pyrimidines as multitarget protein tyrosine kinase inhibitors for the treatment of Idiopathic Pulmonary Fibrosis (IPF). ChemMedChem 15: 182-187.

Sun Q, Hu J, Yu P, Zhu Z, Yu R, Ge C, Li C, Wu G, Lin B, Liu G, Liu M, Bian H, Xu H, Jia S (2019) Peptide PD29 treats bleomycin-induced pulmonary fibrosis by inhibiting the TGF-beta/smad signaling pathway. Exp Lung Res 45: 123–134.

Togami K, Fukuda K, Yamaguchi K, Chono S, Tada H (2018) Facile and sensitive hplc-uv method for determination of nintedanib in rat plasma. Int J Pharm Pharm Sci 10: 133–137.

Togami K, Yamaguchi K, Chono S, Tada H (2017) Evaluation of permeability alteration and epithelial-mesenchymal transition induced by transforming growth factor-beta1 in A549, NCI-H441, and Calu-3 cells: Development of an in vitro model of respiratory epithelial cells in idiopathic pulmonary fibrosis. J Pharmacol Toxicol Methods 86: 19–27.

Wollin L, Maillet I, Quesniaux V, Holweg A, Ryffel B (2014) Antifibrotic and anti-inflammatory activity of the tyrosine kinase inhibitor nintedanib in experimental models of lung fibrosis. J Pharmacol Exp Ther 349: 209–220.

Yamazaki R, Kasuya Y, Fujita T, Umezawa H, Yanagihara M, Nakamura H, Yoshino I, Tatsumi K, Murayama T (2017) Antifibrotic effects of cyclosporine A on TGF-beta1-treated lung fibroblasts and lungs from bleomycin-treated mice: role of hypoxia-inducible factor-1alpha. FASEB J 31: 3359–3371.

Yount SE, Beaumont JL, Chen SY, Kaiser K, Wortman K, Van Brunt DL, Swigris J, Cella D (2016) Health-related quality of life in patients with Idiopathic Pulmonary Fibrosis. Lung 194: 227–234.